BNL-230072-2026-TECH

On the Possibility of Installing the Rapid Cycling Synchrotron of the Electron Ion Collider in the AGS Tunnel

F. Willeke

December 2024

Electron-Ion Collider

Brookhaven National Laboratory

U.S. Department of Energy

USDOE Office of Science (SC), Nuclear Physics (NP)

DISCLAIMER

On the Possibility of Installing the Rapid Cycling Synchrotron of the Electron Ion Collider in the AGS Tunnel

F. Willeke, December 2024

Abstract

This report describes electron injector concepts for the Electron Ion Collider (EIC) using the tunnel of the Alternating Gradient Synchrotron (AGS) of Brookhaven National Laboratory [1] which is to be compared to the RCS in the RHIC tunnel or a new ring in a new tunnel. Possible designs of the electron booster synchrotron, the Rapid Cycling Synchrotron (RCS) with good spin transparency with electron energies of up to 10 GeV and 18 GeV and placing the injector linac in the adjacent Building 912 for are worked out. The main reason for studying such options is the expectation that it will reduce the Electron Ion Collider injector cost because no civil construction is required, the machine is very compact, and existing infrastructure can be used. The design of an RCS with a top energy of 10 GeV with good spin transparency is quite conventional. However, for collider operation with 18 GeV electrons, this option would require accelerating the 10 GeV beam in the Electron Storage Ring (ESR) to 18 GeV and relying on the Sokolov Ternov self-polarization at 18 GeV in the ESR. Solutions for an RCS with Electron energies of up to 18 GeV with or without spin transparency are found to be possible but push the envelope of conventional magnet technology.

1. Introduction

The Electron Ion Collider, presently under construction at Brookhaven National Laboratory is designed for collisions of high energy (5 GeV-18 GeV) polarized electrons with high energy polarized protons (41 GeV-275 GeV) or ions with an electron-proton luminosity of up to L= (10^{33}-10^{34}) $cm^{-2}s^{-1}$. The average spin polarization of both electrons and proton beams (including light ions such as He^{3+}) is expected to be 70% [2].

The electron storage ring (ESR) of the EIC is designed to be operated with 2.5 A at 5 GeV and 10 GeV and with ≈ 240 mA at 18 GeV. The rapid cycling synchrotron (RCS) of the EIC will deliver polarized electron beams for the electron storage ring. It is designed to be operated from its injection energy of 400 to 800 MeV to 5 GeV, 10 GeV and 18 GeV. The polarized electrons will be produced in an existing polarized electron source with a demonstrated polarization of 85% and a bunch charge of up to 11 nC [3]. Electron spin polarization is required to be preserved during acceleration in the RCS.

The original design of the RCS [2] promised a maximum beam energy of 18 GeV, a bunch charge of 28 nC and a cycle frequency of 1 Hz. The bunches of full energy were to be injected into the electron storage ring in a swop-in/swop-out mode enabled by a fast kicker magnet so that every bunch can be replaced every 6 min on average. This original version of the RCS has been abandoned due to a number of problems, many associated with the limited space in the RHIC tunnel that houses the two collider rings.

Several solutions for acceleration of polarized to 10 GeV and 18 GeV in an RCS accommodated in the AGS tunnel are worked out as a lower-cost alternative to an RCS in a new not yet existing tunnel.

In the first, lowest-cost version, the RCS will accelerate polarized electrons to 10 GeV. In this case, acceleration of electrons up to 18 GeV would occur in the ESR. Polarization of 18 GeV electron beams in the ESR would rely on the Sokolov-Ternov self-polarization with a maximum polarization of ~70%. Simulations show [4] that electron polarization of up to this level will be possible at 18 GeV in the ESR and can be reached after 20 min of storage at 18 GeV.

A second solution provides electron beam energies of up to 18 GeV, but polarized beams would be limited to 10 GeV. No acceleration in the ESR would be necessary but spin polarization at 18 GeV would still depend on the Sokolov-Ternov in the ESR.

The third option that is discussed would provide polarized electron beam up to 18 GeV. This option has high demands on the magnet system.

The machine is designed for a total charge of 28 nC, possibly distributed over four or more bunches.

The advantage of the RCS in the AGS tunnel is a substantial cost saving by using existing tunnels and buildings and possible sharing of accelerator infrastructure.

The cost saving will arise from:

- No, or minor civil construction cost
- The smaller size of the ring
- Limiting the injector linac energy to 400-800 MeV
- The usage of Bld 912 next to the AGS tunnel for housing a 400 MeV commercial s-band linac
- Bld 912 will be able house most of the equipment of the RCS
- The liquid 2K Helium of the RF test stand will be able to provide coolant for at least one 5-cell s.c. cavity which is sufficient for 10 GeV of beam energy.
- Sharing of the transport line from the AGS to the EIC tunnel with hadrons.
- Sharing of existing infrastructure such as the existing spare power supply with energy storage of the AGS.

There are also cost disadvantages such as

- Larger RF voltage and RF power needs due to the smaller bending radius
- A long injection line for injection into the storage ring

that need to be considered in a cost comparison.

The purpose of this report is to show possible solutions and discuss their feasibility, technical choices, and to provide a preliminary cost estimate.

1. Constraints and Boundary Conditions

The design of the RCS in the AGS tunnel must meet several requirements:

- The RCS must fit into the AGS tunnel
- The RCS should remain close to the outer wall to avoid reducing the distance between the AGS and the RCS for providing sufficient passage. This implies a close to circular shape of the RCS.
- The RCS should not block any access to the AGS tunnel and not obstruct any access to egress ways.
- The RCS lattice should have a periodicity of at least 24 and up to 42 and should have a vertical integer tune of larger than 24 for 10 GeV and 42 for 18 GeV operation
- The magnetic elements of the RCS should remain within conventional magnet technology to maintain the cost advantage of building the RCS in the AGS tunnel
- Number of power supplies should be minimized to avoid excessive cost
- The bend radius should not be larger than 50 m to limit the RF voltage requirements at the peak energy

The designs presented in this report will meet these requirements.

2. Accelerator Lattice of the 10 GeV version of the RCS

In the following, we will describe the 10 GeV version. The 18 GeV options will be discussed in the later sections of this report.

The AGS tunnel has a circular shape with a radius of 131.81 m at the outer tunnel wall (circumference 828.2 m). The circumference of the RCS is chosen to be 824.14 m. The average distance between the beam orbit and the outer tunnel wall is 64.5 cm. The ring is composed of 24 identical super-periods. Each super period is 34.154 m long. A super-period contains 4 $^1/_2$ FODO cells that are 6.831 m long plus a half cell with a 3 m long straight section. These straight section half-cells are with L = 3.6 m some 18.5 cm longer that the regular FODO half cells. These straight sections that will accommodate rf cavities as well as injection and extraction pulsed magnets reduce the lattice periodicity to 24. The radial variation of the beam orbit is small and varies only slightly between -7.3 cm and + 4 cm with respect to the average radius.

There is space for 9 dipole magnets of 1.765 m length (hard edge magnetic) in each super-period. The corresponding bending radius is 60.691 m, which corresponds to an injection dipole field of 220 Gauss (400 MeV) and a maximum field of 5.5 kGauss at 10 GeV beam energy. Thus, to operate with an injection field of 300 Gauss, injection energy of 546 MeV is required (there is space for a LINAC with a beam energy of at least 800 MeV).

Focusing is provided by the 60 cm long quadrupole magnets (hard edge magnetic) with a gradient of up to 26.2 T/m. The FODO cell contains also two sextupole magnets of 30 cm length with a strength of up to 260 T/m^2, and two, 15 cm long dipole correctors which need a field of 0.2 T to produce a 1 mrad kick at 10 GeV (corresponding to 13 mm closed orbit deviation or a quadrupole misalignment of 2.5 mm).

Figure 1 shows two segments of the accelerator lattice relative to the AGS tunnel walls (the AGS itself is omitted from these plots). All elements are shown with a width of 60 cm in of this plot.

A list of the lattice elements and their parameters is shown in Table I. The AGS tunnel cross section is shown in Figure 2. The cross section of a preconceptual design of the RCS dipole is shown close to the outside wall. The RGS is assumed to be installed above the level of access- and egress-opening of the tunnel that are all on the outside wall avoiding any obstruction of these important passages. However, the RCS stays clear of the tunnel crane which must remain operable. The high vertical position also will help to avoid interference with AGS injection and extraction lines. See Figure 2 that depicts the tunnel cross section.

The 64 cm distance of the RCS design orbit from the outer tunnel wall leaves space for cable trays, extra space for superconducting cavities, allows to leave existing electrical distribution panels in place, and preserves access to the tunnel emergency stop "crash-cord" the outer tunnel wall, such that the personal safety systems remain untouched.

Details of the RCS in the areas of AGS injection are not shown at present. This part of the tunnel requires a careful detailed study. The RCS ring can be azimuthally arranged (rotated) to optimize the arrangement for injection and extraction as well as liquid 2 K Helium supply for superconducting cavities. A super period has only a 15-degree azimuth angle and a length of 34.154 m.

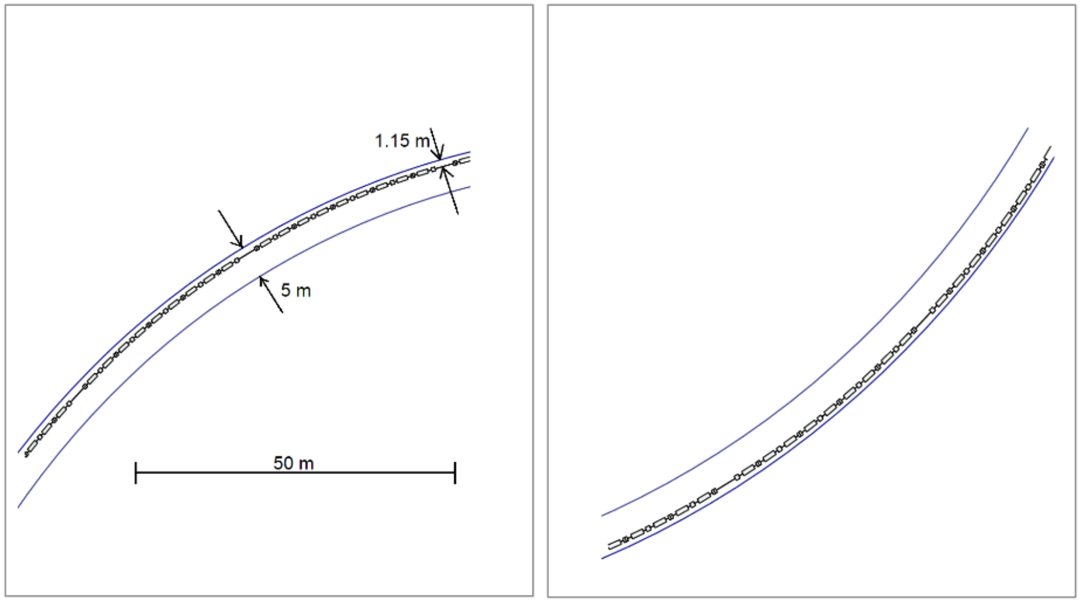

Figure 1: RCS lattice Segments with AGS tunnel wall segments, the distance of the beam orbit to the wall is 64 cm an average. Radial variation around the ring remains within 10 cm.

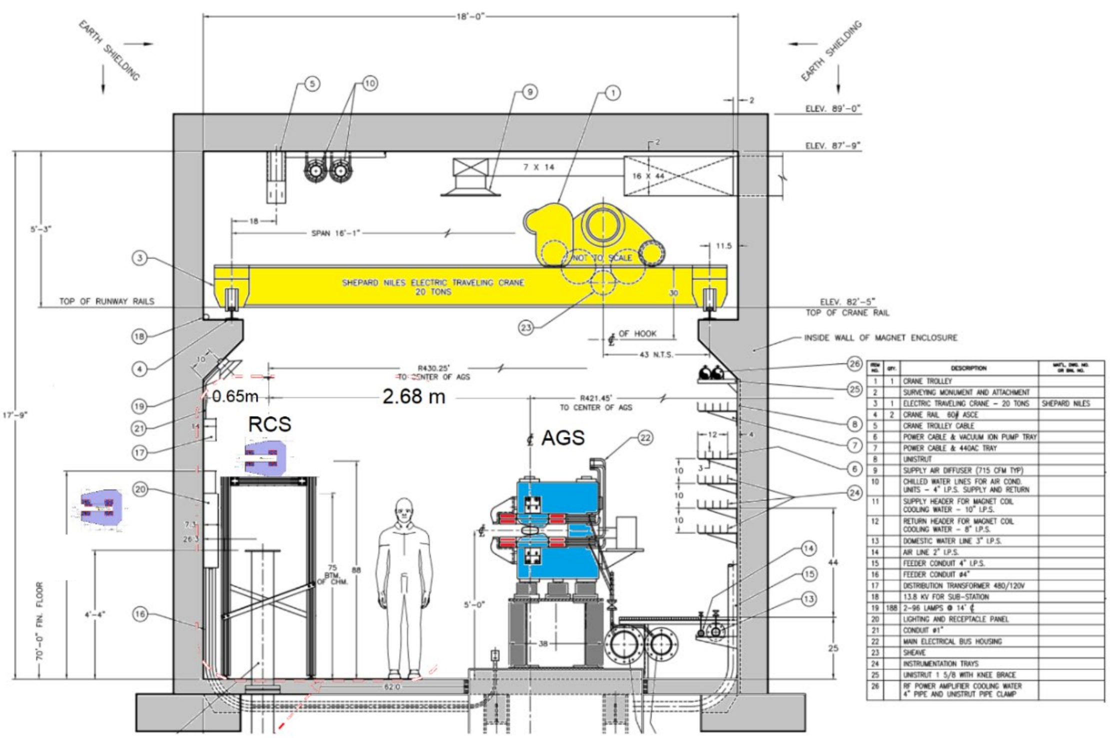

Figure 2: The RCS cross section in the AGS tunnel. The RCS is shown on the left side, the AGS on the right side. The layout allows for a s.c. RF cavity-cryostat diameter of up to 1.2m. There is flexibility in the design to move the ring somewhat further away from the outer wall should that be necessary. The presented layout ensures that the RCS can be installed using the AGS tunnel crane (shown in yellow). Conclusion at this point is that on a first look the AGS tunnel offers enough space, width and headroom to accommodate a 10 GeV RCS, including supports and cable trays. Potential interferences with AGS injection, extraction and RF systems appear to be solvable and no major equipment needs to be moved out of the way.

3. Beam Optics and Beam Dynamics Parameters of the 10 GeV Solution

The beam optics has a periodicity of 24 (thus 24 periods) which is essential for good polarization performance up to 10 GeV. The beam optics of a super-period is a FODO lattice with 4 1/2 complete cells and a half cell with a 3 m long straight section between the adjacent quadrupole magnets.

The quadrupole magnets are powered by a focusing quadrupole and a defocusing quadrupole circuit. Four quadrupoles of the super-period, the ones closest to the long straight section are assumed to be powered independently (or powered using correction coils or have slightly different yoke lengths) to match the 3 m straight section to the regular FODO cell. They differ by about 5% in strength of the regular horizontally focusing and vertically focusing FODO quadrupoles. The beam optics is nearly regular with maximum beta functions < 13.5 m.

Table I: Lattice Parameters

Parameter	Unit	Value
Design Injection Energy	[GeV]	0.40
Design Beam Energy	[GeV]	10.00
Average Distance of Orbit from AGS outer Wall	[cm]	64
Number of Super-Periods		24
Number of regular cells per super-period		4.5
Number of dipoles in the lattice		216
Number of quadrupoles, sextupoles, correctors		240
Number of utility straight sections per super period		1
Length of the Super-period	[m]	34.15
Length of regular FODO cell	[m]	6.831
Length of long straight section	[m]	3.00
Length of the Dipole	[m]	1.765
Bend Radius	[m]	60.691
Magnetic Dipole Field at Design Energy	[T]	5.50
Magnetic Dipole Field at Injection Energy	[Gauss]	220
Length of the Quadrupole Magnet	[m]	0.60
Maximum quadrupole Gradient	[T/m]	26.20
Maximum k-value	[m^{-2}]	0.78
Length of the Sextupole Magnet	[m]	0.30
Maximum Sextupole field Strength B_2	[T/m^2]	260
Maximum sextupole strength m=1/2ecB''/E	[m^{-3}]	16.67

Dipole corrector length	[m]	0.15
Dipole corrector field	[T]	0.22
max. Dipole Corrector kick at Design Energy	[mrad]	1.
Distance between elements	[m]	0.15

The dispersion is not matched but has a periodicity of 24 and is only 10 cm in the long straight. The horizontal betatron phase advance of a super period is close to 488 degrees. Therefore, the missing effect of the missing dipoles on the dispersion function partially cancels pairwise. The maximum dispersion is 43 cm. Dispersion matching and reducing the peak dispersion can be easily achieved by two more independent quadrupole circuit which is kept as an option at this point. The momentum compaction factor is rather large with $\alpha_{mc} = 1.46 \cdot 10^{-3}$ which has an impact on the required RF amplitude. It might be a good cost trade off to better match the dispersion, reducing the momentum compaction factor and reducing the required RF voltage which could reduce the cost for the RF cavities. On the other hand, the dispersion as presented provides a horizontal beam emittance of close to the required 20 nm for extraction into the ESR. The question of how to optimize the dispersion is left to a future stage of optimization.

The regular FODO cell has a phase advance of $\Delta\phi_x = 0.26 \cdot 2\pi$, and $\Delta\phi_y = 0.215 \cdot 2\pi$ (subject to further optimization and fine tuning). The ring tunes are $Q_x = 32.557$ and $Q_y = 25.301$, both also being subject to further optimization. Figure 3 shows the matched beam optics over six super periods.

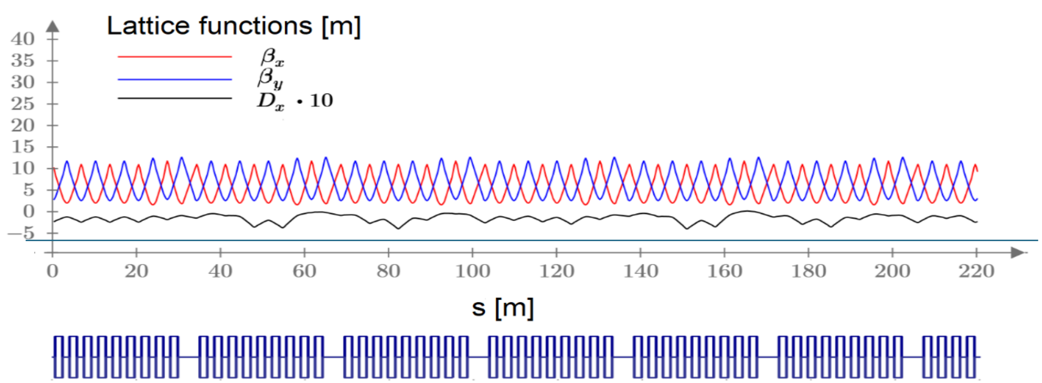

Figure 3: Beam optics parameters, the beta functions in both planes and the dispersion function, over six super-periods. The box structure indicates the positions of dipole magnets. The vertical scale is meters. Note that the dispersion is shown with a multiplication factor of 10.

The natural chromaticities are $\xi_x = -39.38$ and $\xi_y = -33.081$. Chromaticity correction to $\xi_{x,y} = +1$ in both planes requires integral sextupole strengths of $S_x = -3.87$ m^{-2} and $S_y = 3.876$ m-^{2} which correspond to sextupole fields of $B_2 = 220$ Tm^{-2} (note that the sextupole field is defined as $B_2 = d^2B/dx^2$ excluding the factor of 2 needed when using a Taylor expansion).

These are modest values that promise good dynamic aperture values (not evaluated at this point).

Due to the relatively small value of the bend radius $\rho = 60$ m, the electron energy loss at 10 GeV is 14.61 MeV which is quite large (at 18 GeV, this would be 153.4 MeV). This large energy loss is the price to pay for a lattice that meets perfectly all conditions for good spin transparency and the provision of sufficient space for superconducting cavities in the straight section. The damping times are well partitioned with 3.77 ms transversal and 1.88 ms longitudinal. The beam emittance is calculated as 16.3 nm nm, slightly lower than the 20 nm emittance value of the electron storage ring but easily adjustable by lowering the horizontal tune or alternatively, if a rf frequency offset of $\Delta f_{rf} \approx 40$ kHz (which moves the orbit inside the quadrupoles by up to 4 mm) is applied. A list of beam dynamic parameters is compiled in Table II.

Table II Beam Optics Parameters

Parameter	Unit	Value
horizontal tune		32.56
vertical tune		25.31
max/min horizontal β-function in cell	[m]	11.42/1.99
max/min vertical β-function in cell	[m]	11.41/1.99
max/min horizontal dispersion in cell	[m]	0.106/0.03
max β_x	[m]	11.72
max β_y	[m]	12.72
max dispersion	[m]	0.43
Average Dispersion in long straight	[m]	0.05
Momentum compaction factor	[10^{-3}]	1.16
Hor. natural chromaticity		-39.4
Vert. Natural chromaticity		-33.1
Equil. Horiz. Beam Emittance (10 GeV)	[nm]	16.3
Energy loss per turn	[MeV]	14.61
damping time τ_x	[ms]	3.76
damping time τ_y	[ms]	3.76
damping time τ_s	[ms]	1.88
beam energy spread (10 GeV)	[10^{-3}]	1.10

4. Polarization Performance

The lattice and beam optics provide favorable conditions for the preservation of spin polarization during the ramp. The high lattice periodicity of 24 and the large vertical integer tune of >25 should suppress all intrinsic depolarizing resonances up to the extraction energy E_{max} = 10 GeV. A preliminary spin tracking study was performed to explore the evolution of the spin during the ramp. The vertical tune was chosen Q_y = 24.03. For the simulation, the particle is launched on a betatron trajectory with an oscillation amplitude of 2.5 σ_y (σ_y is the standard deviation of the vertical beam size). The beam emittance is assumed to be constant during the ramp with ε_y =7 nm. The normalized emittance at injection is assumed 5 μm, thus ε_y =6.25 nm and 50% of the horizontal equilibrium emittance at 10 GeV is ε_y = 8 nm. Tracked is only one particle with its initial spin pointing in the vertical direction.

The spin direction for such a 2.5 sigma betatron amplitude particle is not much affected for the most the ramp and indication of a stronger impact is only seen at the spin tune of ν_{sp} =22 (E=9.68 GeV) with extraction at ν_{sp} =22.7. More systematic tracking with multiple particles, possibly including radiation effects and optimization of the vertical tune is required for a complete assessment of the polarization on the ramp with systematic resonances. Figure 4 shows the vertical component of the spin of a single particle when considering systematic depolarization resonances (closed orbit assumed to be zero) between injection energy (400 MeV) and extraction energy (10 GeV).

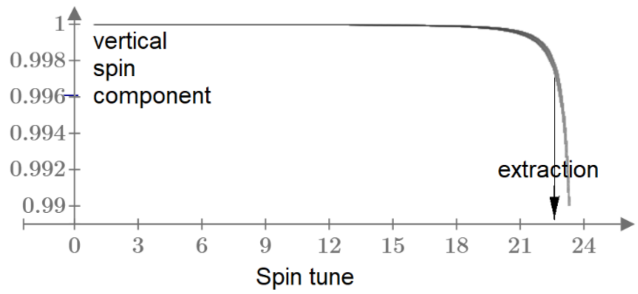

Figure 4: Polarization performance between injection and extraction with systematic resonances. Vertical tune is 26.3, ramp speed is 5 T/s, betatron amplitude is 0.9 mm (2.5 σ_y). Tracked is one particle starting with vertical spin component of one.

A preliminary study has also been performed on the impact of imperfection resonances.
The quadrupole magnets are assumed to be aligned with a precision in the order of a fraction of a millimeter, δy_{rms}= 0.3 mm. This is well within the state of the art and should be achievable in a ramping accelerator. The corresponding orbit deviations have a rms value of Δy_{rms} = 5.6 mm. The orbit can be well corrected with corrector kicks in the order of a few hundred μrad to rms values of about Δy_{rms} = 1.4 mm.
Figure 5 shows the corrected vertical orbit and the corresponding vertical kicks in the quadrupole magnets and dipole correctors. The kicks from the residual orbits in the quadrupoles and the adjacent correctors are added. Their rms value is 0.6 mrad.

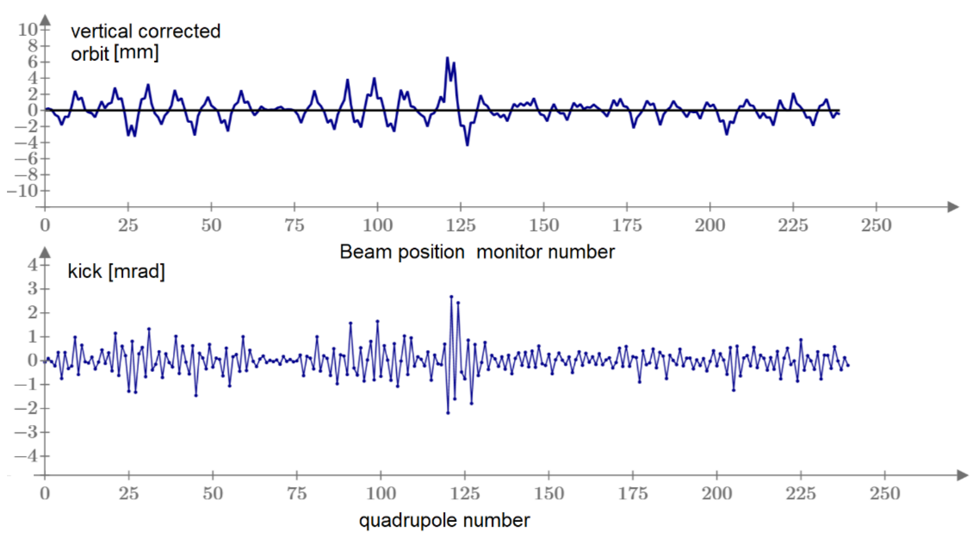

Figure 5 Corrected closed orbit and corresponding distribution of vertical kicks in the quadrupole magnets

A single particle with initial spin pointing in the vertical direction has been tracked between injection and extraction. A corrector is placed next to each quadrupole. The result is shown in Figure 6.

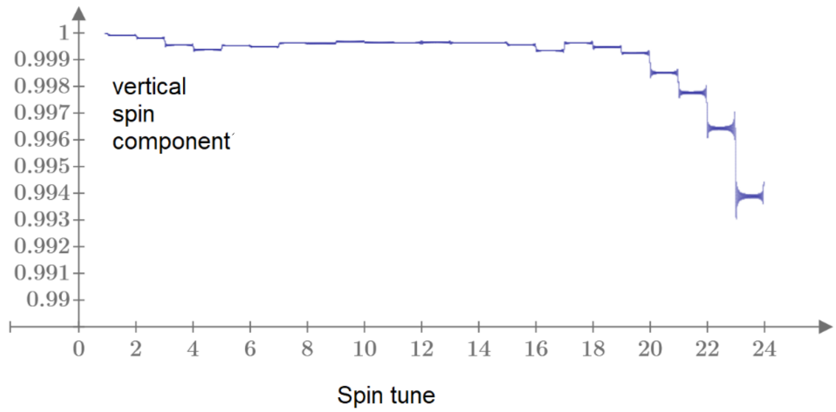

Figure 6 Vertical spin component of a single particle on the ramp between injection and extraction with imperfections. After correction, rms value of the residual closed orbit is 1.4 mm, the rms vertical kick 0.6 mrad, the ramp speed is 5 Tesla/s .

Figure 7 shows the situation when systematic kicks from a vertical betatron oscillation and the kicks from the correctors are applied simultaneously.

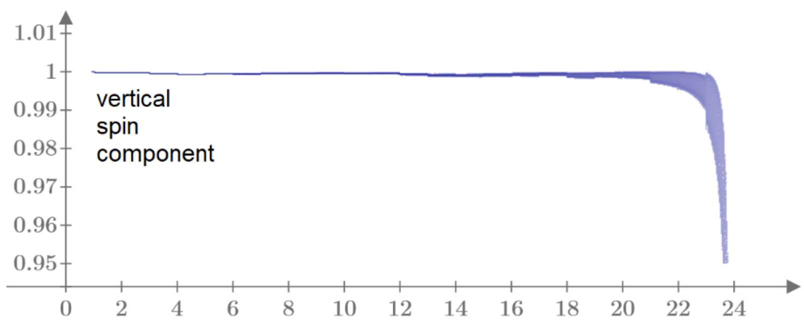

Figure 7: Spin tracking with both systematic and nonsystematic errors, same parameters as described above

Conclusion polarization performance: The study results in a good preservation of the electron spin polarization on the entire ramp. The strongest resonance occurs at $\nu_{sp} = 22$ which causes a depolarization of ≈1 percent. However, the presented study is preliminary and incomplete. Simulations need to be calculated with many particles and more systematic variation of to obtain a more reliable assessment. Nevertheless, it appears to be possible to achieve an acceptable spin transparency (polarization > 99%) with the lattice presented. However, inspection of the results of spin tracking suggests that a lattice periodicity of >24, let's say 25 would have an even better suppression of the spin resonance 22. This would require a periodicity of 25. The space for RF cavities would shrink to 2.9 m, the quadrupoles and dipoles would become 4% stronger which would require increasing the circumferential voltage of the RF system.

5. Radiofrequency System

The lattice provides a 3 m long straight section in each of the 24 super-periods. These straight sections will house RF cavities and other equipment such as kicker, septa, etc. This straight section is long enough for a single cell 591 MHz cavity.

The energy loss of a 10 GeV electron in the RCS is 14.71 MeV. The rms energy spread at 10 GeV is $(\Delta E/E)_{RMS} = 1.106 \cdot 10^{-3}$. To accommodate $10 \cdot (\Delta E/E)_{RMS}$, the synchronous phase must be limited to 42.2 degrees to provide a good RF lifetime at top energy which requires at least 2 x 6 sigma of the energy spread. Note that the longitudinal damping time is less than 2 ms and beam lifetime will be affected if the bucket area would be too small. An RF voltage of 21.8 MV is thus required to compensate for beam energy loss and to provide sufficient RF bucket height. The synchrotron frequency is 8.01 kHz which is a reasonable value.

The beam current in the RCS is only 10 mA (assuming 28 nC of charge accelerated), and the corresponding peak RF power loss is only 148 kW. It is assumed that this power can be easily provided by solid state amplifiers which is the assumed RF power source.

The EIC single cell 591 MHz superconducting cavity fits into the 3 m long straight section provided by the lattice (see Figure 6) with some minor modifications. The long tapers that are required to maintain stability of the high intensity ESR electron beams can be shortened somewhat. Such cavities can reach an accelerating gradient of 20 MV/m. With an active length of 25.4 cm, 4 single cell cavities are required to achieve the desired voltage of 22.9 MV.

The supply of 2 K liquid He for the superconducting cavities can be provided by the cryogenic plant that provides cryogens for the ESR superconducting cavity test facility that is located in building 912, closely to the AGS tunnel. Thus, no extra cryogenic plant is required for the RCS superconducting cavity.

The resulting bucket height is 1.12% which provides about 10 times the RMS energy spread of 10^{-3}. Figure 7 shows the corresponding longitudinal phase space. Table III summarizes the RF parameters.

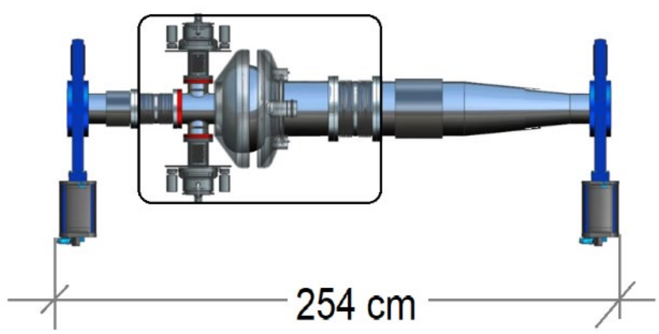

Figure 7: Modified version of the EIC single cell superconducting cavity. The taper is slightly steeper than in the high beam current version for the ESR and so is the right hand-side distance between cavity and the warm-cold transition.

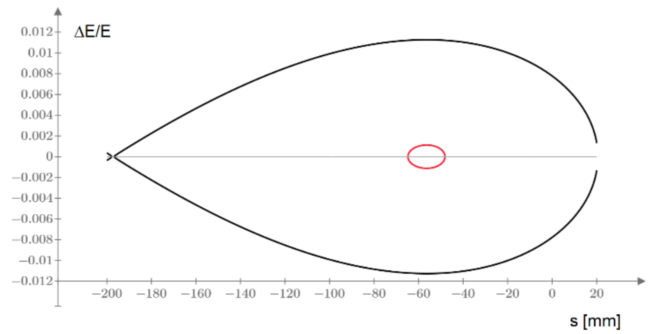

Figure 7: Longitudinal phase space with 5 single cell 591 MHz superconducting cavities and a synchronous phase angle of -40 degree. The black trace is the separatrix that peaks at ΔE/E=11%. The red trace represents the RMS beam envelope with $\Delta E/E_{RMS}=10^{-3}$ and a bunch length of approximately 8 mm. The bucket height is approximately 7 $\cdot \Delta E/E_{RMS}$.

The conclusion regarding the rf system is that the overall parameters appear reasonable and the system can be implemented with available RF technology. It is however, somewhat unfortunate that a single 5-cell superconducting cavity would not fit in the available straight section. Straight sections would need to be approximately 1 m longer. This can be accomplished while preserving the ring periodicity on the expense of a shorter dipole, enhanced synchrotron radiation losses, more and stronger individually powered quadrupole magnets. The quest whether the present simple solution is the best compromise needs further investigation.

Table III RF Parameters

Parameter	Unit	Value
RF frequency	[MHz]	591.00
Harmonic number		1611.00
RF Voltage	[MV]	21.8
Accelerating Gradient	[MVm^{-1}]	20
Energy loss per turn	[MeV]	14.71
Synchronous phase	[degree	43.00
RF power	[kW]	110
Momentum compaction factor	[10^{-3}]	1.11
Number RF cells/cavity		1
Number of s.c. cavities	[m]	4
Synchrotron frequency	[kHz]	8.01
Bunch length (rms)	[mm]	7.6
Beam rms energy spread (10 GeV)	[10^{-3}]	1.11
Bucket height /energy spread		6

6. Magnet System

The RCS lattice has a conventional layout with 216 dipole magnets, 240 quadrupole magnets, 240 sextupole magnets, and 240 horizontal and vertical dipole correctors.

6.1 Dipole Magnet and Circuit

The dipole magnet of an electron machine is preferable a C-magnet with a C-shaped yoke to avoid exposing the coil to synchrotron radiation from the beam. The lattice provides space for a dipole length of length 175.4 mm. The sagitta is only +/- 3.2 mm, thus the magnet can be made straight.

With a bend radius of 60 m and a beam energy of 10 GeV, the required maximum dipole magnetic field is B = 0.553 T.

With an emittance of 24 nm, the horizontal RMS beam size is W_{beam}=0.71 mm. This value includes the off-energy part of the beam size. We assume that a provision of D_{xco}= 5 mm for closed orbit deviations is sufficient (the beam size at injection is small). There is some provision for injection errors that are assumed to be Δx_{inj}= 10 mm for on-axis injection. With these assumptions, the beam requires of 44 mm of radial space in the magnet gap. The distance of the beam edge from the pole edge is assumed to be 30 mm to ensure good field quality. Making provisions for the sagitta, this results in a pole width of ~108 mm. The cross section of the two magnet pancake coils is 30 mm times 60 mm (see below). To avoid saturation, a modest maximum B field of 0.7 T is assumed in the yoke. This requires a maximum yoke thickness of 65 mm. The total magnet width is then W_{magn} = 300 cm.

The maximum rms vertical beam size is 0.5 mm, and 10 sigma of the beam is 5mm. Here we assume a vertical emittance half the horizontal one, ~8 nm. The space for closed orbit error in the vertical direction is assumed to be 10 mm but the injection error is assumed to 3 mm. The distance of the 10-sigma beam envelope from the pole is assumed to be 10 mm. These considerations are consistent with a gap height of 47 mm and a total magnet height of 237 mm.

These numbers are the result of estimates using generally accepted formulae, but the validity of the estimates must be confirmed by numerical magnet field calculations

The magnet current averaged over the magnet coil cross section that results from the gap height of 47 mm, and the field of 0.553 T is 22 kA applying Gauss' law and assuming high-μ carbon steel. OFE Copper is assumed as the coil material. As these dipoles are ramped, a slightly aggressive value of the current density of 5 A mm^{-2} in the conductor can be assumed which results in a required coil area of 3420 mm^2. To minimize cost, two 'pancake' coils are foreseen with a cross section of 64 mm x 32 mm which includes 1mm of insulation around each of the four 30mm x 30 mm conductors assuming implies four magnet windings, two for each of the two pancake coils.

Each conductor carries 4.275 kA. The coils need to be water cooled. The cooling channel cross section inside the conductor is 0.8 times the conductor width which leaves a conductor area of 425 mm^2. The total conductor length of the pancake coils is 17 m. Figure 8 shows the cross section of the dipole magnet.

The area of the cross section is 0.044 m^2 and given the length of 175.4 mm, the volume is 0.0153 m^3. Thus, the weight of the yoke is 604 kg. The copper fraction of the coil conductor area is 0.00045 m^2. The copper volume of the conductor is 0.0076 m^3. The weight of the coil is thus 67.3 kg. The entire magnet weighs approximately 675 kg.

A sketch of the yoke is shown in Figure 8.

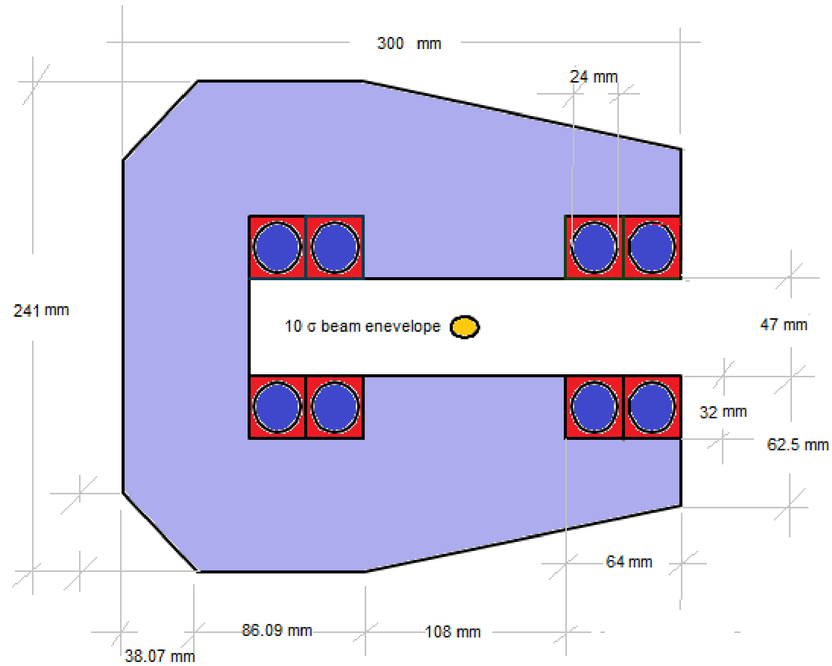

Figure 8: Preliminary layout of the dipole magnet: Cross section of the dipole magnet

6.2 Quadrupole Magnet:

There are 240 quadrupole 60 cm long magnets in the lattice. These quadrupole magnets are laid out for a maximum gradient of 26 T/m. They are represented in the lattice by a 0.6 m long hard-edge quadrupole element. The pole radius of the strawman design is 23.5 mm, three times the horizontal 10· σ_x beam size. The magnet has ten windings per coil and requires a peak magnet current of 1100 A. The yoke is composed of two halves. The coils have only one layer so they can be assembled on a half-yoke. This increases the achievable mechanical accuracy of the magnet. The coils are 7.6 cm long and they are 7 mm thick (values without insulation). The current density of the conductor has been assumed to be 6 Amm^{-2} and the maximum magnet current is 952 A. The total width of the magnet including yoke clamps is ~33 cm. The height is ~28 cm. This magnet is subject to further optimization. Figure 9 shows a possible cross section of the quadrupole magnet.

The quadrupole magnet has the following parameters:

Length	60 cm (hard edge magnetic)
Width	30 cm
Height	24 cm
Quadrupole Field	26 T/m
Pole radius	23.5 mm
Pole width	28 mm
pole tip field	0.149 T
coil size	(8 · 7.6 mm) x (2· 7.6 mm)
current density	10 A mm^{-2}
Magnet current	950 A

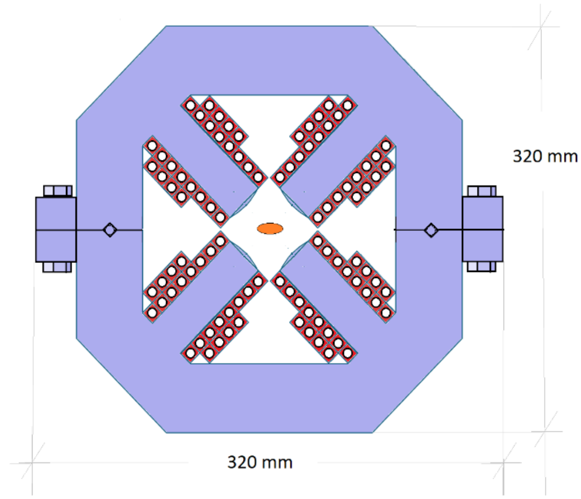

Figure 9 Sketch of the quadrupole cross section

6.3 Sextupole Magnet

The sextupole magnet has the following parameters:

Length	30 cm (hard edge magnetic)	
Width	28 cm	
Height	24 cm	
Sextupole Field	260 T/m	
Pole radius	24 mm	
Pole width	20 mm	
pole field	0.149 T	
coil size	5 x 10 mm^2	
current density	1.8 A mm^{-2}	(no water cooling required)
Magnet current	179 A	

It is assumed that the upper and lower pole can be removed to ease the coil installation. Figure 10 depicts the cross section of the sextupole magnet

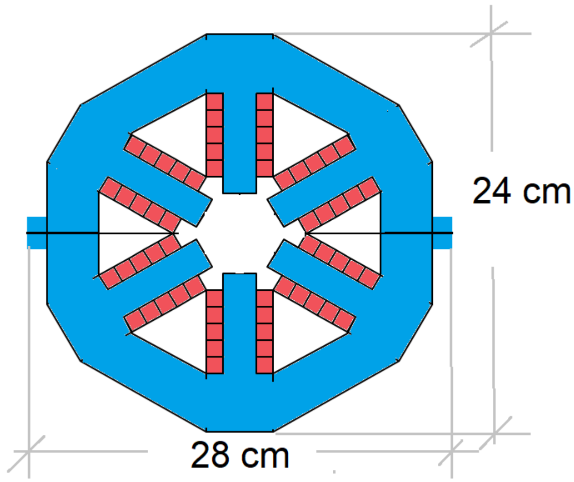

Figure 10: Cross section of the sextupole magnet

6.4 Dipole magnet circuit:

The magnet circuit with 216 dipole magnets and a 15 mm return cable radius then has a resistance of 0.278 Ω at room temperature. The maximum voltage across the magnet power supply at top excitation is 1.19 kV. The magnet as described has an inductivity of 99 μH and the entire ring has an inductivity of 21 mH. We assume a sinusoidal magnet excitation with 1 Hz cycle frequency and find the maximum PS current of 4.37 kA, the maximum PS voltage of 1.9 kV and the maximum instantaneous power consumption of 5.286 MW. The average power consumption of the cycle is 2 MW. Some type of energy storage for this power circuit is advisable to minimize the load on the grid. As RCS and AGS do not have to run in parallel for AGS mutual disturbances should be small. The possibility of sharing the AGS fly-wheel power storage for the RCS should be investigated (the AGS has a second "spare" power supply and spare fly wheel).

Figure 11 shows graphs of these values versus time.

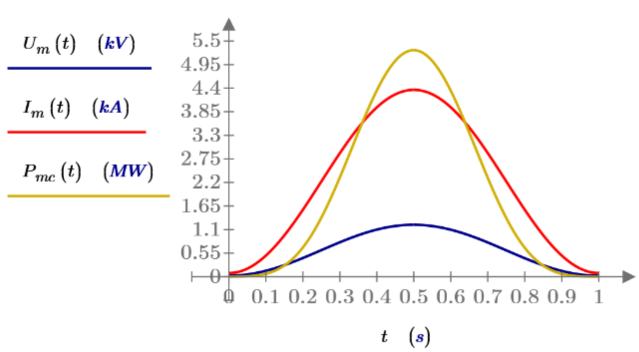

Figure 11 Dipole circuit parameters during the cycle, blue trace power supply voltage in kV versus time, magnet current in kA vs time, and instantaneous power consumption in MW vs time.

6.5 Possible further simplifications of the magnets

Possible savings include combining the horizontal and vertical correction coil in one magnet and shorten the horizontally focusing sextupole magnet by ~20%. This would allow to lengthen the dipole magnet by ~25%. These potential cost saving are not realized in the presented lattice. Another option is to shift the quadrupole magnets, QF and QD in opposite direction in the order of 5 mm to help with bending. This could further reduce the bending strength by 8%. All these measures would reduce the required voltage by ~30% reducing the number of super conducting cavities from five to four.

It is worth mentioning that these modifications of the lattice would allow to achieve a maximum beam energy of 18 GeV requiring 100 MV which could be obtained by 22 superconducting single cell cavities each providing 5 MV. The layout of the magnets would have to be modified accordingly (this is discussed in section 12.

7. Pre-injector and Injection and Extraction

The 400-800 MeV injector LINAC will be carried over from the existing injector design. The pre-injector fits comfortably in hall 912B. The tunnel vault required for radiation shielding can be composed of existing concrete shielding that provided radiation shielding of the external SGS beam lines for High Energy fixed target physics. The layout of the 400 MeV LINAC needs to be slightly changed to make optimum use of the available space, and the relative position of klystron gallery and laser room need to be modified. It would also be advantageous to rotate the spin into the vertical position using a Wien-filter as recently been worked out. Figure 12 shows a preliminary layout for the purpose of show the relative size of the existing Building 912 complex, the AGS tunnel and the 400 MeV version of the linac. The presently planned bunch compressor and spin rotator would not be needed for this design as the bunch intensity is envisioned to be only 1 nC.

The presently laid out LINAC could be shortened as it was previously planned to be operated with only 10 MV/m which could be doubled, thereby reducing the length of the LINAC to about 40 m or alternatively double the injection energy.

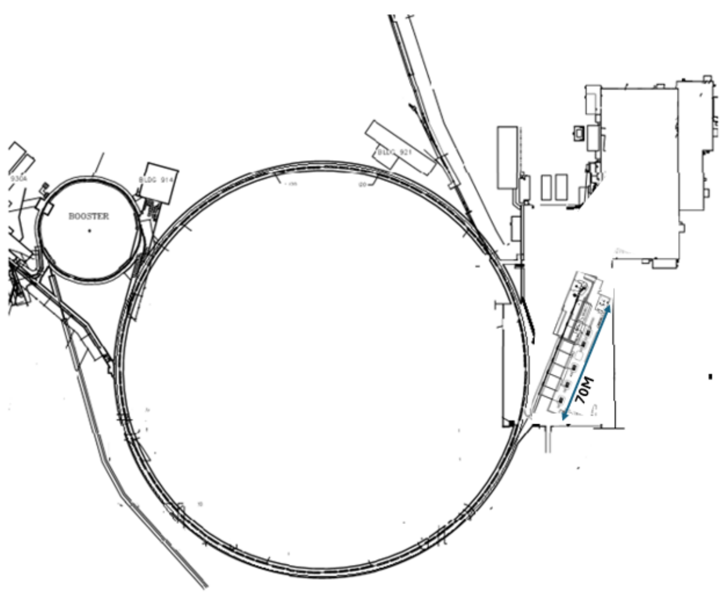

Figure 12: Possible position of a 400 MeV injector LINAC in building 912 adjacent to the AGS tunnel

8. Transfer lines

Hadron injection and electron injection do not occur at the same time. This provides the opportunity to use the EIC hadron injection line to transport the RCS 10 GeV beam from the AGS tunnel closer to the EIC tunnel reducing thereby significantly the electron high energy transfer line cost for dipole and quadrupole magnets as well as vacuum chamber and beam diagnostics cost.

9. Vacuum System

The vacuum chamber can be made of stainless steel with round pipes of 45 mm diameter and a wall thickness of 0.4 mm. Each vacuum chamber extends over a half FODO cell (3.4 m) with a bellow at the end connected to its neighbor by stainless steel conflat flanges (quadrupole supports can be lowered so that the vacuum chamber can be inserted). Pumping is provided by one integrated ion getter pump per FODO half-cell. Two gate valves are required around each of the s.c. cavities. The vacuum section which corresponds to a super period is separated by isolation valves.

10. Cost estimate

This is a preliminary top-down estimate. The basis of estimate is mostly professional judgement and, in some cases, recent vendor responses for similar systems. Cost will need revisiting going to a greater level of detail. Table IV provides an overview of cost numbers. There are no overheads assume for procurements. Cost numbers are given without escalation in 2024 dollars. Labor costs are fully burdened in 2024 $. The cost number is 188 M$. More details of the cost estimate are given in Table IV.

11. 18 GeV Option

It is possible to accelerate electron beam to 18 GeV in an RCS installed in the AGS tunnel. The 18 GeV lattice has a bend radius of 70.7 m which requires a larger injection field for an injection field of 280 Gauss. The dipole field at 18 GeV is 0.85 T. This option thus comes with a 600 MeV injector linac. The lattice is now composed of 54 L = 15.259 m long alternating gradient focusing cells which are all identical and the super-periodicity is 54. The distribution of bending magnets over the cell is strongly asymmetric. There are two 3.29 m long dipoles in one half-cell and only one 1.645 m long dipole in the second one. The second half-cell contains also a corrector magnet for both transverse planes. and two quadrupole magnets and a 4.94 m long straight section that is large enough to accommodate a 5-cell superconducting cavity. The sextupole magnets are integrated into the dipole pole profile. There is space for additional sextupoles in the long straight sections that are not required otherwise. The vertical betatron phase advance per cell is 0.407 $\cdot 2\pi$ and the adjustable tunes are $Q_x = 21.9$, Q_y=22.3. The beta functions are rather large and peak at ~53 m. The peak dispersion is 0.685 m. The natural beam emittance is rather large, $\varepsilon_x = 140$ nm at 18 GeV and ε_x= 40 nm at 10 GeV. The rms energy spread of the 18 GeV beam is $1.8\cdot10^{-3}$. The beam optics is depicted in figure 13. The natural chromaticities are $\xi_x = -56$ and $\xi_y = -57$. The integrated sextupoles are assumed to be 1 m long and have a modest strength of less than 35 T/m^2.

Table IV Cost estimate for the 10 GeV only version

TOP-Down Cost Estimate	2024 $	
LINAC and Particle Source	**40**	M$
Magnet System	**21.1**	M$
196 dipole magnets a 35 k$	7	M$
220 quadrupole magnets a 30 k$	6.6	M$
220 sextupole magnets a 25 k$	5.5	M$
196 Corrector magnets a 8 k$	2	M$
Power Supplies	**18**	M$
1 dipole supply 5 kA, 1 kV	5	M$
2 quadrup. suppl. 1 kA, 1 kV	5	M$
2 sextup. suppl. 0.4 kA, 0.5 kV	2	M$
196 Corrector supplies, 50 A, 10 V a 5 k$	1	M$
Cables	5	M$
Transfer lines	**15**	M$
RF System	**16.5**	M$
Cavities, 5 single cell 591 MHz s.c. cav. A 3M$	15	M$
RF power, 250 kW, 6 $/W	1.5	M$
Vacuum system	30.36	M$
Vacuum chamber 800 m 1000$/m	**15.18**	M$
24 bellows a 10000 k$	0.24	M$
240 flanges a 1500 $	4.8	M$
240 ion pumps and pump controller a 10000	2.4	M$
10 fast gate valves a 50 000 $	0.5	M$
24 isolation valves a 10k$	0.24	M$
Vacuum controls and interlock,	5	M$
Miscl	2	M$
Pulsed Magnets	**5**	**M$**
Diagnostic and Controls	**20**	M$
Labor for design, assembly and installation, 3 y, 50 FTE/y 250k$/FTE	**37.5**	M$
Total	**188.28**	M$

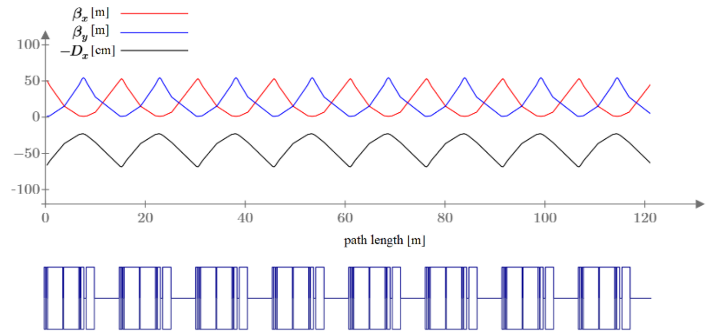

Figure 13: 18 GeV RCS lattice in the AGS tunnel. There are 54 focusing cells with a strongly asymmetric distribution of the bending magnets. One half-cell has two 3.29 m long dipoles , the other half cell has one 1.65 m long dipole. The box structure indicates the position of the magnetic elements. The long straight section is 4.93 m long.

The dipole magnet requires a larger pole width and a larger coil as the 10 GeV magnet. The weak sextupole component of the dipole can be rather easily implemented in the pole design. The coil area of dipoles and quadrupole magnet approximately doubles and the overall magnet dimensions change from 30 cm height and width to 60 cm height and width. This magnet is still well within the limits of a conservative design.

The quadrupole magnets are 60 cm long and require a gradient of 26 T/m which is still a conservative choice.

The beam energy loss per turn at 18 GeV is 131 MeV (12.5 MeV at 10 GeV). An RF voltage of 200 MV will provide a bucket height of six times the rms energy spread. This requires 8 five-cell superconducting 594 MHz cavities with an accelerating gradient of 20 MV/m which can be accommodated in the long straight sections. Only one five cell cavity is needed for 10 GeV operation. The parameters of the 18 GeV lattice are summarized in Table V.

The polarization will be preserved up to 10 GeV. Figure 14 shows the spin transport to 10 GeV in presence of imperfections corresponding to a quadrupole misalignment of 0.3 mm and a vertical betatron amplitude of 3 σ_y. The polarization will be flipped at 10 GeV and is assumed to not survive the ramp up to 18 GeV. This however, should be investigated further. Polarization for 18 GeV polarized beam collisions still needs to be built up after injection into the ESR by the Sokolov-Ternov effect. Ramping of the ESR would not be required.

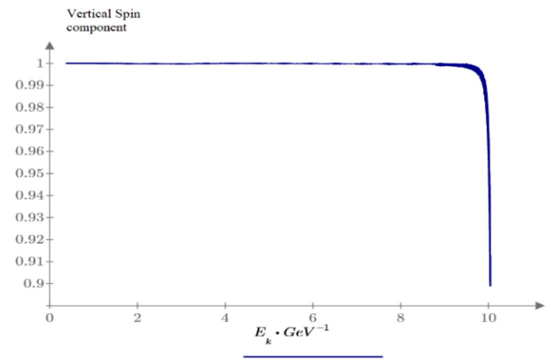

Figure 14: Vertical spin component on the RCS ramp up to 10 GeV for a particle with an 2.5 sigma betatron amplitude and a corrected closed orbit of 2 mm.

Compared to the dedicated 10 GeV option discussed in the previous sections, the cost for magnets would increase by a factor of approximately 2 by about 20 M$. The cost of the power supplies capable of 18 GeV operations would increase by 18 M$. One interesting option would be to use the available AGS fly-wheel which would save substantial power supply cost. The RF cost for 10 GeV operation would be reduced by 4 M$. Thus, the initial investment for an 18 GeV option would be a total cost of 220 M$ compared to the 10 GeV only version of 188 M$. Note that this is a very crude estimate.

Table V: Parameters of the 18 GeV lattice with polarization up to 10 GeV

Parameter	Unit	Value
Maximum Beam Energy	[GeV]	18
Circumference	[m]	824
Number of super periods		54
Number of alternating focusing cells per super period		1
Lengths of the dipole magnets	[m]	3.29 , 1.645
Max. Strength of the dipole magnet	[T]	0.85
Number of dipoles		108, 54
Length of the quadrupole magnet	[m]	0.6
Number of quadrupoles		108
Strength of the quadrupole	[T/m]	26
Length of the integrated sextupole magnet	[m]	1
Number of sextupoles (integrated into the long dipoles)		108
Strength of the sextupole	[T/m^2]	35
Number of x-y Correctors		54
Length of the long straight section	[m]	4.93
Beam Energy loss at 10, 18 GeV	[MeV]	12.55, 131.7
RF Voltage for 6 σ bucket height, 10 GeV, 18 GeV	[MeV]	21, 200
Number of cavities required for 10 GeV, 18 GeV		1, 8
RF peak power at 10 GeV, 18 GeV for 28 nC charge (10 mA)	[MW]	0.125, 1.32

12. RCS in the AGS Tunnel: An Option with Polarization at 18 GeV

An RCS option for acceleration of up to 18 GeV is quite challenging but not impossible. While the option discussed in the previous section has already the required periodicity, a version with a larger tune closer to $Q_y \approx 41$ will result in a good polarization performance up to 18 GeV. However, it requires a more challenging magnet system. This option is discussed in this section.

A circumference of 820 m is chosen. The maximum beam energy is 18 GeV. The injection energy is 800 MeV. The lattice has a super-periodicity of 42. The super-period is 19.52 m long. It has a straight section of 4.5 m which will accommodate the RF cavities and four alternating gradient focusing cells composed of two alternating gradient combined function dipoles. Each focusing cell is 4.88 m long. The length of the combined function magnets is L = 1.547 m. The sextupoles are integrated into the combined function bending and focusing magnets. These parameters correspond to a bending radius of ρ = 82.7 m which results in a fill factor of 63.4%. The bending field at 18 GeV is 0.72 T and at 800 MeV injection energy it is 320 Gauss. Each focusing cell has one corrector for both transverse planes. The gradient of the dipole field is 35 T/m. There are 8 combined function magnets in the lattice. The 8th magnet is split into two halves that are located on each side of the long straight section. There are 6 double-plane correctors in each super-period. The lattice functions over three super-periods are shown in Figure 15.

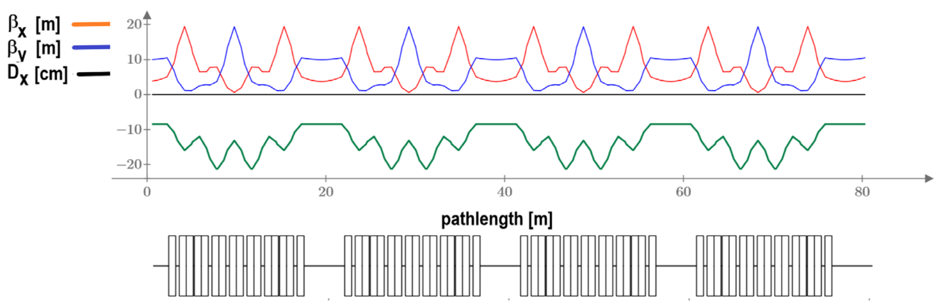

Figure 15: Lattice functions over three of 42 super-periods are shown. The large straight sections will accommodate 5-cell 594 MHz superconducting RF cavities, inject and extract elements and additional vertically focusing sextupoles.

It should be noted that as there is sufficient of straight section space, additional correctors and defocusing sextupoles can be placed in most straight sections that are not occupied by RF cavities or injection and extraction elements.

The tunes of this lattice are Qx=32.8, Qy=40.29. The natural chromaticities are ξ_x = -57.9 and ξ_y =-58.6. With the horizontal dispersion between 10 cm and 20 cm, their compensation requires a sextupole component of -75 T/m^2 and -88 T/m^2. Additional, vertically focusing sextupoles in the available straight sections will reduce these values.

The horizontal damping time is only little affected by the combined function lattice. It is still about 1ms at top energy of 18 GeV. The horizontal beam emittance is ε_x = 20 nm at 10 GeV and ε_x = 68 nm at 18 GeV. These values can be further optimized. The 10-sigma beam envelope is within 12 mm (assuming a 50% vertical to horizontal emittance ratio).

The with a bending radius of ρ = 82.7 m, the beam energy loss at 18 GeV is relatively low with 112.6 MeV and an RF voltage of 159 MV provides a bucket height of 5 σ_e for enough beam lifetime at extraction. Six

5-cell superconducting cavities with an accelerating gradient of 20 MV/m are required to provide this voltage. The beam energy spread is $1.68 \cdot 10^{-3}$ and the bunch length at extraction is 5.9 mm. The synchrotron frequency is 15.7 kHz. Figure 16 shows a rendering of the EIC 5-cell cavity [6].

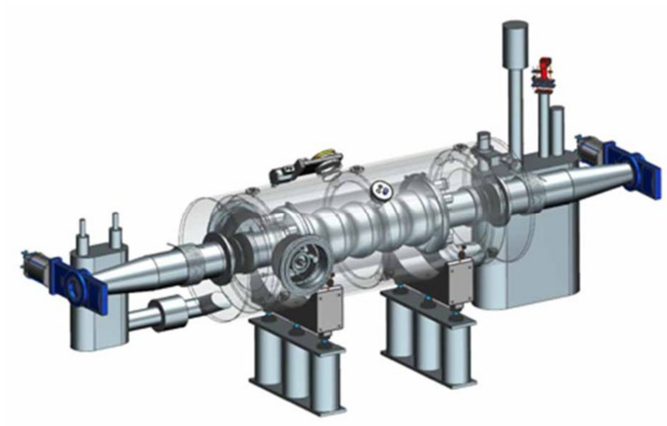

Figure 16: Rendering of the EIC 5-cell 594 MHz superconducting cryomodule copied from reference [6]. Considering the low beam and bunch current for the RCS, the tapers on both ends can be shortened by 15 cm so the the cryomodule fits into the available straight section space of 4.5 m.

The parameters of the lattice for polarization of to 18 GeV are shown in Table 6.

Compared to the 18 GeV solution with polarization up to 10 GeV, no substantial cost increase is expected. The increased cost of the combined function magnets is in part compensated by the elimination of extra quadrupoles and the somewhat reduced number of RF cavities and RF power. We can assume a cost of about 230 M$ for this solution.

Table VI: Parameters of the 18 GeV lattice with polarization up to 18 GeV

Parameter	Unit	Value
Maximum Beam Energy	[GeV]	18
Circumference	[m]	820
Number of super periods		42
Number of alternating focusing cells per super period		4
Lengths of the dipole magnets	[m]	3.29, 1.645
Max. Strength of the dipole magnet	[T]	0.73
Number of dipoles		108, 54
Length of the quadrupole magnet	[m]	0.6
Number of quadrupoles		108
Strength of the quadrupole	[T/m]	26
Length of the integrated sextupole magnet	[m]	1
Number of sextupoles integrated into the long dipoles		108
Strength of the sextupole	[T/m^2]	35
Number of x-y Correctors		54
Length of the long straight section	[m]	4.5

Beam Energy loss at 10, 18 GeV	[MeV]	12.55, 131.7
RF Voltage for 6 σ bucket height, 10 GeV, 18 GeV	[MeV]	21, 200
Number of cavities required for 10 GeV, 18 GeV		1, 8
RF peak power @ 10GeV, 18GeV, 28 nC (10 mA)	[MW]	0.125, 1.32

Polarization:

With a periodicity of 42 and a vertical tune close to 40, the polarization performance up to 18 GeV is good. Figure 18 shows the vertical spin component on the ramp from 800 MeV to 18.4 GeV including corrected closed orbit (rms value 2.4 mm) due to 0.3 mm magnet misalignment. Even with residual orbit distortions of several millimeters, the polarization transparency is acceptable. Improved orbit correction is expected to improve polarization performance.

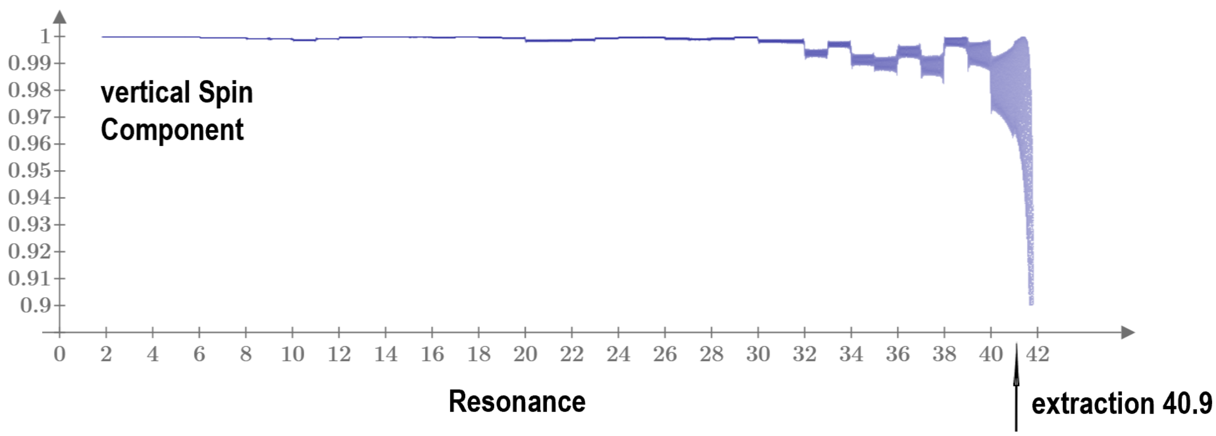

Figure 17: Vertical spin component on the ramp from 800 MeV to 18.4 GeV including corrected closed orbit (rms value 2.4 mm) due to 0.3 mm magnet misalignment. Close to the extraction point at 18 GeV, the vertical spin component is reduced to 97%.

Magnets:

The combined function magnets that are needed for this lattice are still within the state of the art of iron dominated magnets. Because of the strong quadrupole component required, the magnets are designed as half quadrupoles with a mirror plate. The chosen magnet concept while having been implemented in storage rings successfully [see HERA] is certainly not common.

The parameters of the pre-conceptual design of these magnets are:

Design concept:	Half quadrupole with a mirror plate
Dipole field at 18 GeV:	0.726 T
Maximum quadrupole field at 18 GeV:	33.6 T/m
Magnet width:	31.4 cm
Magnet height:	44.9 cm
Offset central beam position from the mirror plate:	21.5 mm
Good field region:	10mm x 13mm (10 sigma plus 3mm closed orbit)
Pole radius:	36.5 mm

Pole tip field	1.25 T
Number of coil windings	10
Coil dimensions	15 mm x 15 mm
Current density of the conductor	8 A mm^{-2}
Magnet current at 18 GeV:	1790 A
Pole width:	56.3 mm
Thickness of the return yoke and the mirror plate	90 mm
Magnetic field in the return yoke	0.6 T
Cooling	water cooled conductor

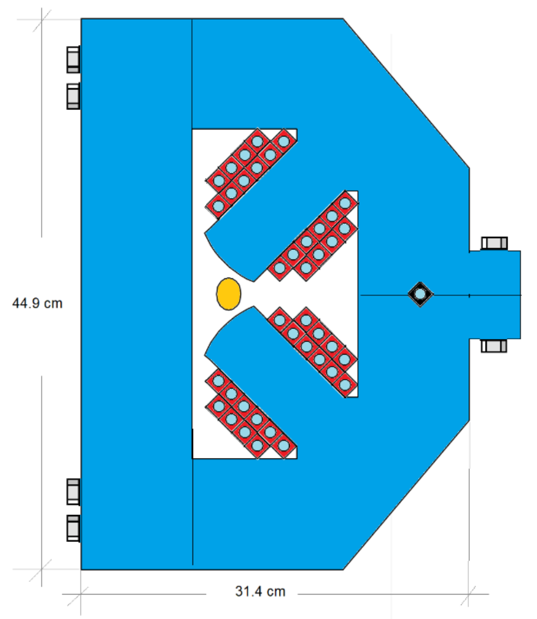

Figure 16: Sketch of the cross section of the combined function magnet for up to 18 GeV operation with polarization transparency over the whole energy range. The half quadrupole has a gradient of up to 33.6 T/m and a dipole component of 0.73 T at the beam center which is at a distance 21 mm from the mirror plate. The pole radius is 36.5 mm. Some of the magnets have a sextupole component as well which is obtained by a special shape of the pole face. The yellow circle corresponds to 10 σ of the transverse equilibrium rms beam size at 18 GeV including a 3 mm margin for closed orbit distortions

13. Conclusions

The study of a 10 GeV rapid cycling synchrotron installed in the existing AGS tunnel does not reveal any showstoppers or major issues at the modest level of detail considered so far. While many details still need to be considered, putting a 10 GeV RCS into the AGS promises to be feasible, meets all the requirements for 10 GeV beams, observes all the constraints listed at the beginning this report and promises a significant cost advantage as compared to other solutions.

Going 18 GeV Beam energy, however, is somewhat more difficult, however still possible with conservative approaches of accelerator hardware. This however requires a substantial increase of the RF cost.

The first solution for 18 GeV that has been explored suppresses only depolarizing resonances up to 10 GeV. The systematic spin resonances above 10 GeV will not be suppressed, thus 18 GeV operation with polarized electrons would still rely on Sokolov-Ternov self polarization in the ESR art 18 GeV. This is still a considerable advantage compared the 10 GeV solution.

If one wants to commit to somewhat less common (though not unproven) magnet designs, a solution for 18 GeV with parameters for polarization up to 18 GeV is possible as well.

All solutions presented here have been produced in a very short time span with a minimum of resources. Should any of these options considered for constructing the RCS, a substantial amount of work must be invested to improve and optimize the design, to work out a preliminary design of the components, and to address many aspects of the design that have been omitted in the studies present here.

The overall conclusion is that the construction of the RCS in the AGS tunnel is feasible and offers many possibilities to save cost. More detailed design work must be performed to better understand the performance of the AGS-based solution compared to a completely new design of the RCS with a new tunnel and infrastructure without the constraints that go along with using existing structures.

13 Acknowledgement

I am obliged to the EIC design team, in particular to Joseph Tuozzolo, Vahid Ranjbar, Kevin Smith and John Skaritka for many discussions and help with figures.

14 References

[1] AGS
[2] EIC CD1
[3] Polarized electron source

[4] 18 GeV self-polarization
[5] HERA lumi upgrade

[6] Rimmer, R. A., Daly, E., Guo, J., Henry, J., Matalevich, J., Wang, H., Wang, S., Holmes, D., Smith, K., Xu, W., Zaltsman, A., Xiao, B., De Silva, S. U., & Delayen, J. R. (2023). Cavity and cryomodule developements for EIC. In M.E. Biagini, J. Chrin, M. Giabbai, M. Iungo, & V.R.W. Schaa (Eds.), Proceedings of the 65th ICFA Advanced Beam Dynamics Workshop on High Luminosity Circular e+e- Colliders eeFACT2022 (pp. 125-130) JACoW. https://doi.org/10.18429/JACoW-eeFACT2022-WEXAS0101

Appendix I Lattice File for the 10 GeV Solution with a periodicity of 24

Name	length [m]	1/rho [m^-1]	K [m^-2]	S [m^-2]
IP	0	0	0	0
QFH	0.3	0	-0.74349	0
CD	0.225	0	0	0
CX	0	0	0	0
CD	0.225	0	0	0
B	1.754167	0.016582701	0	0
SD	0.3	0	0	0
SY	0	0	0	4.569
SD	0.3	0	0	0
QDH	0.3	0	0.743485	0
QDH	0.3	0	0.743485	0
CD	0.225	0	0	0
CY	0	0	0	0
CD	0.225	0	0	0
B	1.754167	0.016582701	0	0
SD	0.3	0	0	0
SX	0	0	0	-2.915
SD	0.3	0	0	0
QFH	0.3	0	-0.74349	0
IP	0	0	0	0
QFH	0.3	0	-0.74349	0
CD	0.225	0	0	0
CX	0	0	0	0
CD	0.225	0	0	0
B	1.754167	0.016582701	0	0
SD	0.3	0	0	0
SY	0	0	0	4.569
SD	0.3	0	0	0
QDH	0.3	0	0.743485	0
QDH	0.3	0	0.743485	0
CD	0.225	0	0	0
CY	0	0	0	0
CD	0.225	0	0	0
B	1.754167	0.016582701	0	0
SD	0.3	0	0	0
SX	0	0	0	-2.915
SD	0.3	0	0	0
QFH	0.3	0	-0.74349	0
IP	0	0	0	0
QFH	0.3	0	-0.74349	0
CD	0.225	0	0	0
CX	0	0	0	0
CD	0.225	0	0	0
B	1.754167	0.016582701	0	0
SD	0.3	0	0	0

SY	0	0	0	4.569
SD	0.3	0	0	0
QDH	0.3	0	0.743485	0
QDH	0.3	0	0.743485	0
CD	0.225	0	0	0
CY	0	0	0	0
CD	0.225	0	0	0
B	1.754167	0.016582701	0	0
SD	0.3	0	0	0
SX	0	0	0	-2.915
SD	0.3	0	0	0
QFH	0.3	0	-0.70393	0
IP	0	0	0	0
QFH	0.3	0	-0.70393	0
CD	0.225	0	0	0
CX	0	0	0	0
CD	0.225	0	0	0
B	1.754167	0.016582701	0	0
SD	0.3	0	0	0
SY	0	0	0	4.569
SD	0.3	0	0	0
QDH	0.3	0	0.779579	0
QDH	0.3	0	0.779579	0
CD	0.225	0	0	0
CY	0	0	0	0
CD	0.225	0	0	0
B	1.754167	0.016582701	0	0
SD	0.3	0	0	0
SX	0	0	0	-2.915
SD	0.3	0	0	0
QFH	0.3	0	-0.71959	0
IP	0	0	0	0
QFH	0.3	0	-0.71959	0
CD	0.225	0	0	0
CX	0	0	0	0
CD	0.225	0	0	0
B	1.754167	0.016582701	0	0
SD	0.3	0	0	0
SY	0	0	0	4.569
SD	0.3	0	0	0
QDH	0.3	0	0.760814	0
QDH	0.3	0	0.760814	0
LSS	3	0	0	0
QFH	0.3	0	-0.74349	0
IP	0	0	0	0